A TRIDENT SCHOLAR PROJECT REPORT

NO. 477

Electron Phonon Coupling in Superlattice and Multilayer Systems

by

Midshipman 1/C Andrius V. Bernotas, USN

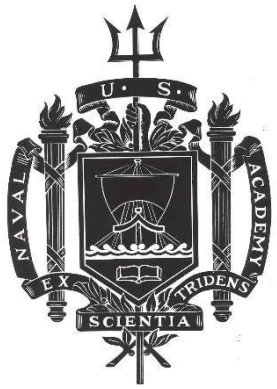

UNITED STATES NAVAL ACADEMY
ANNAPOLIS, MARYLAND

USNA-1531-2

REPORT DOCUMENTATION PAGE

Form Approved
OMB No. 0704-0188

1. REPORT DATE *(DD-MM-YYYY)*	**2. REPORT TYPE**	**3. DATES COVERED** *(From - To)*
5-20-19		

4. TITLE AND SUBTITLE Electron Phonon Coupling in Superlattice and Multilayer Systems	**5a. CONTRACT NUMBER**
	5b. GRANT NUMBER
	5c. PROGRAM ELEMENT NUMBER
6. AUTHOR(S) Bernotas, Andrius V.	**5d. PROJECT NUMBER**
	5e. TASK NUMBER
	5f. WORK UNIT NUMBER
7. PERFORMING ORGANIZATION NAME(S) AND ADDRESS(ES)	**8. PERFORMING ORGANIZATION REPORT NUMBER**
9. SPONSORING / MONITORING AGENCY NAME(S) AND ADDRESS(ES) U.S. Naval Academy Annapolis, MD 21402	**10. SPONSOR/MONITOR'S ACRONYM(S)**
	11. SPONSOR/MONITOR'S REPORT NUMBER(S) Trident Scholar Report no. 477 (2019)

12. DISTRIBUTION / AVAILABILITY STATEMENT

This document has been approved for public release; its distribution is UNLIMITED.

13. SUPPLEMENTARY NOTES

14. ABSTRACT

Multilayer thin films are critical to microelectronics design (for example, as diffusion barriers between the silicon active layer and copper interconnects). However, work is needed to understand potential thermal bottlenecks that could arise from their use in transistors. A major source of thermal buildup in microelectronic devices is the interaction between electrons and the surrounding atomic species when they are in a state of thermal nonequilibrium, through electron-phonon (EP) coupling. In this project, we explore EP coupling in multilayer superlattices and oxide conductors. We use ultra-fast optical measurements of these systems, a numerical solution to the two temperature thermal model, and a graded multilayer thermoreflectance model to better understand the relationship between the EP coupling in these multilayer materials and the physical parameters of the system. We show in this project the validity of using a multilayer two temperature model in understanding thermal diffusion on the time and length scales associated with microelectronics, and we show that in superlattice configurations, the electron phonon interactions within the materials can vary greatly as compared to these interactions in the constituent materials. This change in behavior shows dependence on both the thicknesses of the layers within the superlattice and the individual properties of each layer's material. We additionally demonstrate a thorough method of processing thermoreflectance data, accounting for various changes in thermoreectance throughout the multiple layers of the system and depth of energy deposited. A greater understanding of these dynamics within multilayer systems will allow for greater control of the thermal properties as they relate to the design of the system, in turn leading to increased thermal efficiency in microelectronics in the future.

15. SUBJECT TERMS

Electron Phonon Coupling, Thermoreflectance, Thermal Transport, Microelectronics

16. SECURITY CLASSIFICATION OF:			**17. LIMITATION OF ABSTRACT**	**18. NUMBER OF PAGES**	**19a. NAME OF RESPONSIBLE PERSON**
a. REPORT	**b. ABSTRACT**	**c. THIS PAGE**		50	**19b. TELEPHONE NUMBER** *(include area code)*

U.S.N.A — Trident Scholar Project Report; no. 477 (2019)

Electron Phonon Coupling in Superlattice and Multilayer Systems

by

Midshipman 1/C Andrius V. Bernotas
United States Naval Academy
Annapolis, Maryland

Certification of Adviser Approval

Assistant Professor Brian F. Donovan
Physics Department

Acceptance for the Trident Scholar Committee

Professor Maria J. Schroeder
Associate Director of Midshipman Research

USNA-1531-2

Abstract

Multilayer thin films are critical to microelectronics design (for example, as diffusion barriers between the silicon active layer and copper interconnects). However, work is needed to understand potential thermal bottlenecks that could arise from their use in transistors. A major source of thermal buildup in microelectronic devices is the interaction between electrons and the surrounding atomic species when they are in a state of thermal nonequilibrium, through electron-phonon (EP) coupling. In this project we explore EP coupling in multilayer superlattices and oxide conductors. We use ultra-fast optical measurements of these systems, a numerical solution to the two temperature thermal model, and a graded multilayer thermoreflectance model to better understand the relationship between the EP coupling in these multilayer materials and the physical parameters of the system. We show in this project the validity of using a multilayer two temperature model in understanding thermal diffusion on the time and length scales associated with microelectronics, and we show that in superlattice configurations, the electron phonon interactions within the materials can vary greatly as compared to these interactions in the constituent materials. This change in behavior shows dependence on both the thicknesses of the layers within the superlattice and the individual properties of each layer's material. We additionally demonstrate a thorough method of processing thermoreflectance data, accounting for various changes in thermoreflectance throughout the multiple layers of the system and depth of energy deposited. A greater understanding of these dynamics within multilayer systems will allow for greater control of the thermal properties as they relate to the design of the system, in turn leading to increased thermal efficiency in microelectronics in the future.

Keywords: Electron Phonon Coupling, Thermoreflectance, Thermal Transport, Microelectronics

Acknowledgments

I would like to thank my project advisor Professor Donovan for the three years of lessons and guidance he gave me in my time at the Naval Academy, which culminated in this Trident Project. Thank you to Professors Warzoha and Smith for their help when I wasn't sure what questions to ask, or how to proceed. Finally, many thanks to the Trident Committee and the Office of Naval Research for allowing me to embark on this research project.

Contents

1 Motivation

As electronics have advanced to take on new roles in an increasingly complex world, they have had to adapt. They have gradually taken increasingly pervasive roles in society, now existing pretty much everywhere you could turn. To fulfill these roles, they have had to become progressively smaller, faster, and more efficient. This challenge has been traditionally tackled through increased clock speeds and more densely packed designs, leading to the development of microelectronics with feature sizes of merely nanometers, which operate over picoseconds. For the past five decades, the exponential rate of advancement of electronics has followed *Moore's Law*, the idea that every two years, the number of transistors on a microchip will roughly double, as displayed in Figure 1.[1, 2] In a world where high performance microelectronics have become pervasive in modern life, new challenges have arisen which should be addressed to continue the advancement of this technology.[3]

New avenues to improve the power of microelectronics beyond shrinking of components have opened up in recent years, such as component specialization, improved circuit architecture, and alternatives to silicon based architecture.[4] One particularly pressing area which should be addressed, however, is thermal buildup in modern microelectronics. This is a universal issue in microelectronics that limits the efficiency and capabilities of the systems.

As transistor density moves towards 100 million transistors per millimeter squared, systems generate significant heat through resistive energy losses. If too much of the energy that powers devices is lost as heat, temperatures will rise to the point where they will, in the worst cases, destroy the components of the device, or at least decrease the lifetime and performance of the device. Some current solutions to this problem are improving dissipative cooling solutions, slowing down clock speeds of the electronics, or compensating with better integrated circuit design, but another way forward in this area is to intentionally design the physical microelectronic components to be more energy efficient.[4]

Transistor architecture leads to an electronic current bottleneck near the interface between the silicon active layer and the copper interconnects. This high current density leads to a high density of energetic electrons, which interact with the atoms in the transistor and result in an increase in thermal energy in these regions.[6, 7] A potential component of tran-

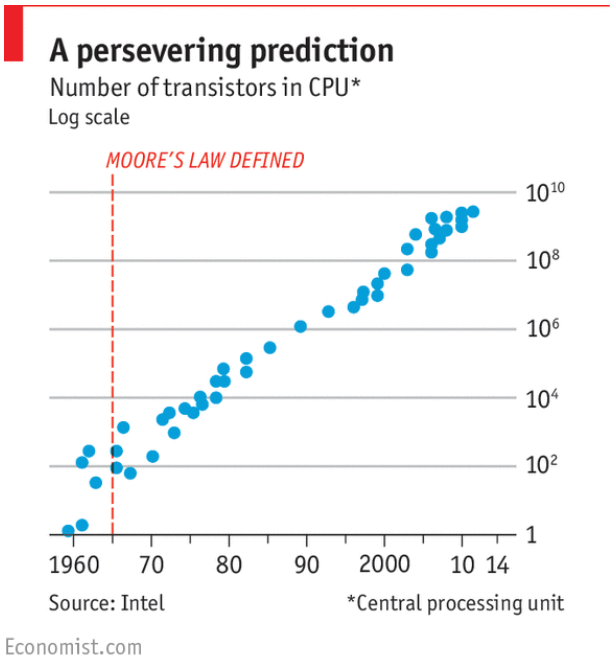

Figure 1: Visual representation of Moore's Law, showing exponential growth in transistor density. [5]

sistors which could be improved to address heat buildup is the diffusion barrier used between the silicon active layer and copper interconnects in the transistor. Without this barrier, precipitates would form between parts of the circuit, degrading efficiency and functionality at a high rate.[8, 9, 10] A simple representation of a transistor, which can turn current flow between the source and drain on or off, can be seen in figure 2, along with the positions of diffusion barriers.

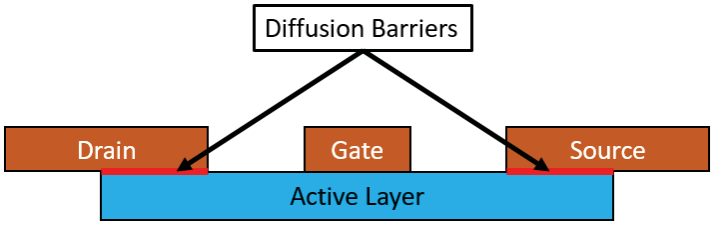

Figure 2: A simple depiction of a transistor, with diffusion barrier locations highlighted for reference.

The ideal diffusion barrier would add no resistance to charge flowing across the silicon copper interface, but it would still prevent material diffusion and degradation. This presents a unique material science and fundamental physics challenge. The industry standard in this regard consists of three metallic materials: tungsten, tantalum, and tantalum nitride.[11, 12, 8, 10] These metallic materials have been found to give good electronic conductivity and stop the diffusion and degradation that would otherwise take place. Currently these materials are placed as a single layers in the transistors, increasing resistance across the boundary in a manner consistent with their characteristic thermal and electronic transport properties.[8]

One proposed improvement to these barriers is utilizing a superlattice with copper in place of a single layer of the material. A superlattice is a periodic, multilayered structure, where alternating layers of different materials are stacked one upon the other. Superlattices are distinguished from other multilayer materials by having a crystal structure that remains consistent throughout the layers of the material. A simplified representation of a superlattice can be seen in Figure 3. Superlattices could produce a system that combines the desirable characteristics of multiple materials, specifically by maintaining characteristics as a diffusion barrier, stabilizing the overall structural stability of the system, and increasing overall cross-plane conductivity.[10, 9] If this can be achieved, it will allow the microelectronics industry to implement a useful advancement to the rapidly developing field of microelectronics.

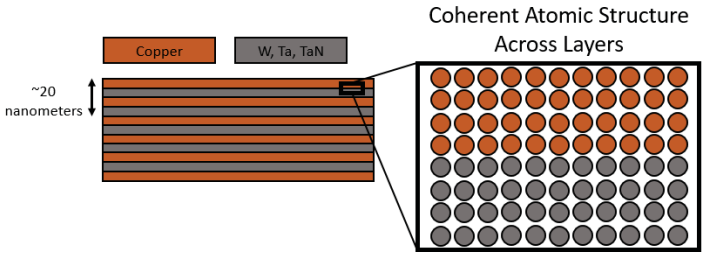

Figure 3: A basic representation of the superlattices we will be considering. Our samples will mainly be in the face centered cubic lattice arrangement, not a square grid as seen in the figure.[12]

An area of study which needs development is the thermal characterization of superlattice systems at the time and length scales at which they would operate in microelectronics. As

current flows through these materials, energy is held in the electrons as they move across a potential difference. In a state where the electrons flowing through the material have significantly more energy than the surrounding lattice, there will be energy transfer from the electrons to the atomic lattice.[13] A focus of this project will be understanding how this energy is thermalized in the lattice of these materials, specifically through energy exchange between electrons and the atoms of the system. This energy exchange occurs through a process known as electron phonon coupling (EP coupling). A comprehensive understanding of how this electron phonon coupling, and the consequent loss of useful energy, is related to the physical design of the system and the thermophysical characteristics of the materials which make up the multilayer system will allow for more intelligent and intentional design of transistors in industry going forward. To this end we employ advanced thermal measurement techniques to experimentally determine the nature of the interaction between electrons and their the atomic lattice for tungsten, tantalum, and tantalum nitride superlattice films. Additionally, we work to advance the thermal characterization methods used in this study to be more applicable to a wider variety of systems in the future.

2 Theoretical Background

As electrons carry charge through a conductor, they will interact with the atoms that make up the material. Through these interactions, the atomic lattice of the material can acquire some energy from the electrons, in the form of atomic vibrations which move through the material. This transfer of energy results in a loss of energy for the electrons and an increase in the thermal energy of the solid. This increase in thermal energy manifests as an increase in temperature over time which is seen in modern microelectronics.[14]

In order to understand these phenomena, macroscopic conceptions of thermal diffusion are not sufficient. The need to extend thermal characterization capabilities into the nanometer length scales and picosecond time scales has pushed the ordinary classical conception of thermal diffusion into a more complex framework, one which accounts for how the energy is actually stored in the material at any given time.

2.1 The Heat Equation

Classical heat flow in bulk materials obeys the relationship known as the heat equation, which describes the flow of energy through a material in time. This is the mathematical conception of the common sense idea that heat flows from hot to cold, until the system reaches a state of thermal equilibrium, which depends on energy sources and boundary conditions specific to the material and scenario in question. This thermal diffusion will always depend on the thermophysical properties of the system in question, and on the geometry of the system in which the heat is flowing.

$$C\frac{\delta T}{\delta t} - \kappa\frac{\delta^2 T}{\delta x^2} = \dot{q} \tag{1}$$

Equation 1 is the heat equation, taught in differential equations courses to describe the diffusion of heat in a system. In this representation C is the heat capacity of the material ($\frac{J}{kg\cdot K}$), T is the temperature (K), κ is the thermal conductivity ($\frac{W}{m\cdot K}$), and $\dot{q}$ is an energy source term (W), describing heat being added to or taken away from the system.

It will be useful to formally define the idea of temperature in this project, for while it is common in everyday life, a uniform understanding will clarify analysis going forward. The best description of temperature for the purposes of this project is that it essentially describes the willingness of one thing to give energy to another thing. Without confusing the issue too much, energy is just a way to talk about the tendency of something to transfer energy to another thermal mass.[15] While this seems like a straightforward concept, examining what is happening in a material on an atomic and electronic scale adds a level of complexity to this idea which is not commonly encountered in everyday life. Combining this idea of temperature and further study of the quantum carriers of thermal energy at these scales will however give a more robust understanding of thermal transport in these systems.

2.2 The Two Temperature Model

The model which has been accepted to help to accurately describe thermal phenomena on picosecond time scales in conductors is known as the Two Temperature Model (TTM). The TTM, as the name suggests, accounts for two temperatures in every material, one of the

phonons in the material and one of the electrons. These two temperatures represent the relative energy transfer tendencies of two interdependent heat carriers. The useful feature of this model is that we are assigning two temperatures to the same physical space. See Figure 4 for an example of 2 temperatures occupying the same physical space.

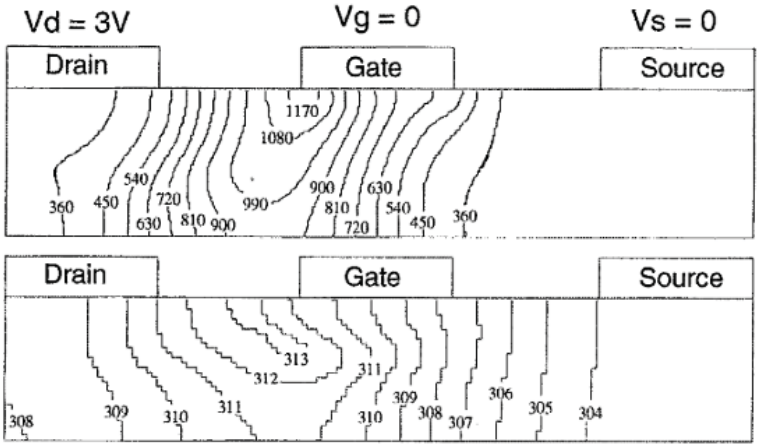

Figure 4: A depiction of a transistor, where the top image shows the electron temperatures, and the bottom image shows the phonon temperatures, at the same time.[6]

At macroscopic limits of time this model behaves the same as the general heat equation, as the two temperatures rapidly come to equilibrium and track as a single temperature. At very short time scales however, on the order of picoseconds, these temperatures can often be different. This is why the need for the TTM exists, so that this non-equilibrium regime, which is consistently present in microelectronics, can be properly accounted for.[16, 17, 18, 13]

The first heat carrier to consider, the phonon, is the nanoscale, quantized version of a vibration in a solid. Atoms in a crystalline solid are bound together through electronic interactions with other atoms. A phonon is a physical displacement which moves through these atoms as a wave. At atomic length scales, these vibrations are well described by quantum mechanics in much the same way that photons are.[19] For both quasiparticles, their energies depend on their frequency and their mobility depends on their momentum and how far they move before interacting with their environment, transferring energy and scattering. The difference between photons and phonons is their medium, as photons, which are quantized packets of light energy, travel through the electromagnetic field, while phonons

travel through a physical medium, the lattice of atoms which makes up physical objects, to include the crystalline nanostructure we are interested in. When considering phonons, the heat capacity and thermal conductivity of the phonon population in a system depends on the available phonon modes, how tightly bound the atoms are, elasticity within atomic interactions, and average scattering rates, among other things. They can also exist in several different states, as optical or acoustic phonons. The phonon specific properties are best determined experimentally in situ, but when not possible there are good approximations and some reported values which can be used to understand the thermal transport in these systems. [20, 21, 22, 23, 24, 25] For the purposes of the TTM though, we assign a temperature to the population of phonons in the lattice, which can change over time and space.

The other heat carrier being considered is the electron. While usually only thought of in the context of being a charge carrier, these particles can carry thermal energy in a material, assuming that material is a conductor. In an insulator this idea is not particularly useful, as the electron population is not free to move and transfer energy. In insulators then, the two temperature model collapses to the single temperature model of heat transfer, and the issue becomes simpler. In conductors however, electrons can attain thermal energy from some disturbance, such as absorption of a phonon or incident photon, or electronic interaction with another electron, and move through the material with the some kinetic energy. In the systems we are interested in, electrons have a fair amount of mobility, which allows them to travel further and carry more energy before scattering, and carry a larger portion of the thermal energy of the material than in insulating materials.[21] In the Two Temperature Model we assign the population of electrons in the material their own temperature, which occupies the same space as the phonon temperature but represents a different set of energetic particles.[23]

The way that the two heat carriers are treated in a similar way in the Two Temperature model is an effect of the particle wave duality that acts both ways when considering both phonons and electrons.[19] The quantum mechanical basis that allows for this statistical mechanics description of these heat carriers is fairly well flushed out, and in these time regimes is a valid and testable way to describe the system.[13] The underlying assumptions about the systems made here are instructive in how to view the heat carriers going forward,

not letting previous conceptions interrupt analysis in the established framework.

2.3 Electron Phonon Coupling

The crux of the TTM is the ability for the two temperatures, of the phonons (or lattice vibrations), and the electrons to interact with each other and exchange energy. This is necessary for the model to physically make sense, and can be achieved by giving each temperature its own heat equation, and coupling them together through a term that is dependent on the difference between the two temperatures at that point in the material.[13] The spatially one dimensional version of these coupled heat equations is represented in equations 2 and 3.

$$C_e \frac{\delta T_e}{\delta t} = \kappa_e \frac{\delta^2 T_e}{\delta x^2} - G(T_e - T_p) + S_1(t) \tag{2}$$

$$C_p \frac{\delta T_p}{\delta t} = \kappa_p \frac{\delta^2 T_p}{\delta x^2} - G(T_p - T_e) + S_2(t) \tag{3}$$

In these equations T_e is the electron temperature, C_e is the electron heat capacity, κ_e is the electron thermal conductivity, T_p is the phonon temperature, C_p is the phonon heat capacity, and κ_p is the phonon thermal conductivity. $S_1(t)$ and $S_2(t)$ are source terms, which are given by energy generated by a source in the system. In our studies, the source term will be omitted in equation 3 because the only significant energy source in our experiments will be light incident on the system. Electromagnetic radiation interacts primarily with the electrons held by the atoms, not the atoms themselves, allowing for this assumption.[21] Finally, and most importantly, G here is the electron-phonon coupling factor, which dictates how the two heat carriers interact in the material, and like the rest of the constants mentioned above, will be dependent on the material which is being considered.

2.4 Thermal Dynamics in a Non-Equilibrium State

The electron phonon coupling factor accounts for the transfer of energy from T_e to T_p and vice versa. This allows a difference in temperature to cause an energy transfer between the carriers, and moves the system towards a state of thermal equilibrium where it matches a single temperature model. This can be understood by viewing it through our conception

of temperature. If the electrons in the system are at a much higher temperature than the lattice, they will be able to reach a more favorable state through transferring energy to the lattice. The ensuing energetic interactions will result in the thermal energy distributed in the electrons decreasing and the thermal energy distributed in the lattice increasing.[26, 27] Thus the temperature difference decreases and will eventually equilibrate, and become a single temperature. This is shown in Figure 5. Once this thermalization occurs, heat transfer occurs like it would in a single temperature model.

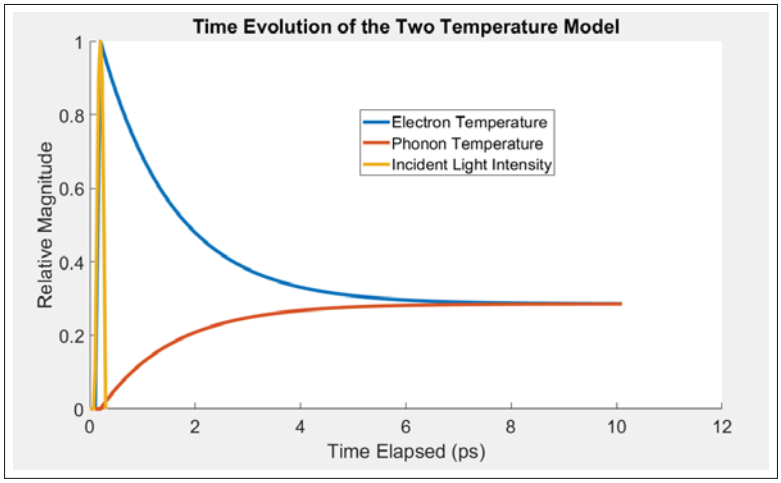

Figure 5: A general overview of how the temperatures will behave in a non equilibrium state, which is in this case induced by incident radiation.

One important thing to point out is just how quickly these two temperatures will move to the same value. In only a few picoseconds, coupling between the electrons and phonons has already occurred to a large extent. Values for this electron phonon coupling factor are generally greater than $1 \cdot 10^{16} \frac{W}{m^3 K}$. With such fast coupling rates, it becomes apparent why this model is not usually necessary to understand other systems.[23]

In a simple one layer system or bulk material, this G can be measured experimentally for a given material. It can be fit as a single value in many materials, with small deviations in temperature.[23] Temperature dependence of the electron phonon coupling factor can emerge over a range of temperatures as well, but G remains well defined as a bulk material property in small temperature deviations. In this project we will be operating with maximum temperature deviations of $< 50K$, which allows this condition to be valid.

This factor becomes more complicated, however, when considering systems other than thin single layers. For example, the addition of material transitions within a sample opens the door to a whole host of complicating factors, including but not limited to contributions of optical and thermal reflections, acoustic effects across the interface, restricted phonon modes, strain waves within the material, and various interactions between heat carriers across the interface.[28]

Quickly then, it becomes apparent that understanding the full effects of electron phonon coupling in systems of increasing complexity is nontrivial. Increasing the fundamental understanding of energy transfer in these systems, where geometry and thermophysical parameters will affect how the transport occurs, is the main focus of this project.

3 Experimental Methods

Investigation of the electron phonon coupling and other thermal dynamics in the microelectronic regime requires highly specialized equipment, which can give subpicosecond resolution measurements of the thermal state of a sample over a heating event. In this project we achieve this through a Time Domain Thermoreflectance (TDTR) experimental setup. We use this setup to study a sample set of superlattices and oxide multilayers of varying layer thicknesses.

3.1 Time Domain Thermoreflectance

Time Domain Thermoreflectance (TDTR) is a characterization method that can be used to measure the thermal properties of materials on the scales of interest, employing an ultra fast pulsed laser to heat a system, and measure the resulting change in reflectance, using the laser pulse itself as a probe.

Reflectance is defined as the intensity of the reflected light divided by the intensity of the incident light ($R = \frac{I_{reflected}}{I_{Incident}}$). As the temperature of a material changes, the electrons in the material and the vibrations in the material lattice change the way that light interacts with the material. This is known as thermoreflectance, where the reflectance of a surface changes due to a change in temperature ($\frac{\delta R}{\delta T}$ or, taking into account the TTM ($\frac{\delta R}{\delta T_e} + \frac{\delta R}{\delta T_p}$)). This is a

well established way to track changes in the temperature of the monitored surface. Within the non-equilibrium conditions studied in TDTR, the thermoreflectance can be governed by a change in both the electron temperature and the phonon temperature of the material, through various modeling methods. By carefully analyzing the change in thermoreflectance from its value from before the pump pulse encountered the surface, we can build a picture of how thermal energy moves through the material. The operational goal of Time Domain Thermoreflectance is to adjust the time delay between when heat is added to a sample and when it's thermoreflectance value is measured, to give a picture of reflectance at different time delays after a heating event. From this signal, information about the electron and phonon temperatures can be gathered.

An experimental setup using a single laser with a split beam, frequency manipulation, and physical time delays allows for this to be achieved. A example schematic of a TDTR experimental setup is included as Figure 6.

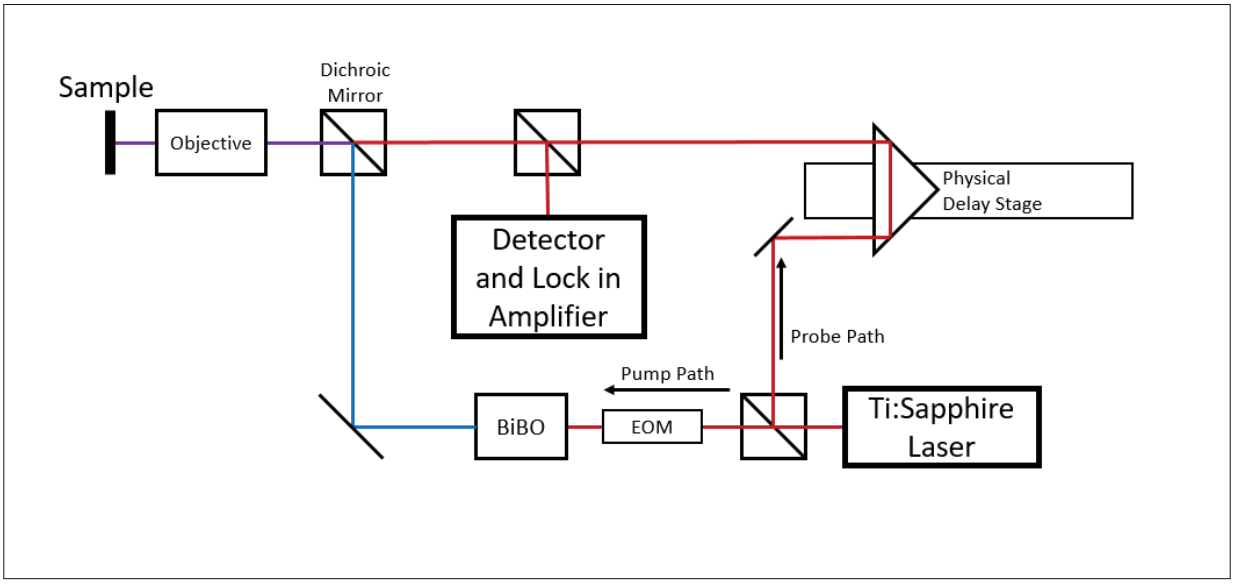

Figure 6: A schematic overview of the a general Time Domain Thermoreflectance optical table setup

The laser used is a Ti:Sapphire Pulsed Laser which is centered around 808 nm wavelength light. This laser produces a beam which is split between two paths upon leaving the laser. The part of the laser light which is to become the pump probe is transmitted through an electro-optic modulator, which modulates the intensity of the laser light pulses at a frequency

of 8.4 MHz. This light is then focused onto a Bismuth TriBorate Crystal (BiBO) which, through a multiphoton absorption event and subsequent emission, depicted in Figure 7, produces light with double the frequency, half the wavelength, and double the energy per photon than the original beam. The purpose of this frequency change is to allow the probe pulse to be able to be isolated effectively, without any feedback from the radiation associated with the pump pulse. After this frequency doubling, the light is filtered of any residual original wavelength light, refocused, and directed to the sample, where it is focused onto the sample by an objective. In Figure 6, this entire process is shown as the lower laser path. This frequency shifted pulse serves as the heating event for the system, depositing energy into the sample.

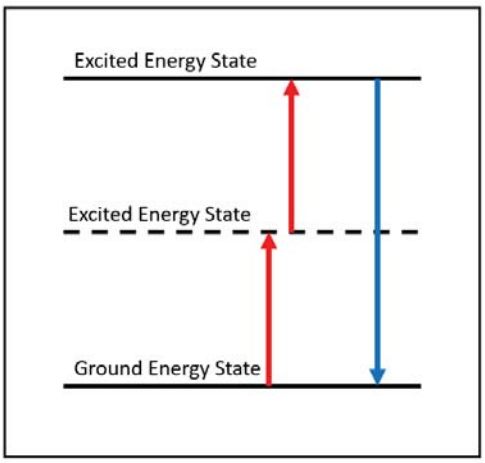

Figure 7: The energy exchange which occurs in the BiBO crystal that allows for the shifting of the radiation frequency. Incoming light has a frequency of 808nm and emitted radiation is at 404 nm.

The other laser path serves as a reflectance probe and is what actually takes the measurement of the reflectance of the sample. Once split off from the pump, the probe beam is directed to an optical delay stage, which can change the path length of the laser and thus the time that it takes for the light to reach the sample. By adjusting the position of the physical delay stage, the probe pulse can be given a positive or negative time delay with relation to the pump pulse. Due to the incredibly small time scales on which the measurements are being taken, the amount of time that it takes light to travel the extra meter which can be

added to the optical path length is enough to get a satisfactory range of time delays. Once the probe pulse has been delayed, it is directed to the sample, where it joins the pump pulse path as it passes through a dichroic mirror, which reflects blue light but will pass red light. At the sample, the probe and pump pulses arrive with the prescribed time delay.

The reflected part of the probe pulse is then passed back through the dichroic mirror, and sent into an optical detector with a lock in amplifier, which isolates and measures only the reflected light from the sample that has a frequency component matching the probe laser. By mapping the energy received by this detector to the time delay of the setup, and varying the time delay over a useful range, a full time domain picture can be constructed of the reflectance of the sample. It is worth noting that these trials are easily repeatable, which allows for statistical averaging of data to ensure that anomalies are not misinterpreted. An example of a TDTR Data set is shown in Figure 8.

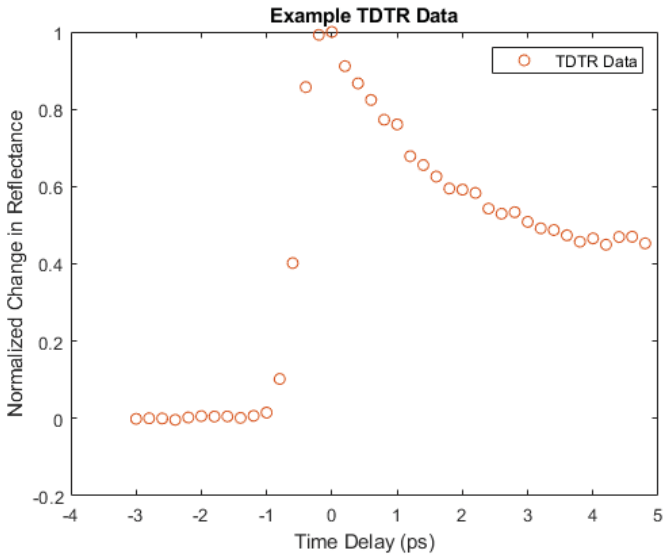

Figure 8: An example of data which is actually obtained in TDTR experiments. This is specifically from a sample of thin film gold on a glass substrate.

3.2 Superlattice Sample Set

Samples were provided by collaborators at Intel and the University of Virginia. In this study, we will take measurements on a variety of copper, tungsten, tantalum, and tantalum nitride

superlattices. The exact set of samples to be tested is described in Figure 9. These samples are varied enough in layer thicknesses and material configurations so as to highlight differing behaviors of interest in the thermal properties of the sample.

Sample	Material 1	Material 1 layer thickness (nm)	Material 2	Material 2 layer thickness (nm)	Number of periodic layers	Total Thickness (nm)
Copper Thin Layer	Cu	95	---	---	1	95
Tantalum Single Layer	Ta	100	---	---	1	100
Tungsten Single Layer	W	45	---	---	1	45
Copper Tantalum Superlattice	Ta	5	Cu	5	25	250
Copper Tantalum Superlattice	Ta	2	Cu	5	15	105
Copper Tantalum Superlattice	Ta	5	Cu	10	7	105
Copper Tantalum Nitride Superlattice	TaN	5	Cu	5	25	250
Copper Tantalum Nitride Superlattice	TaN	2	Cu	5	15	105
Copper Tantalum Nitride Superlattice	TaN	5	Cu	10	7	105
Copper Tungsten Superlattice	W	5	Cu	5	100	1000
Copper Tungsten Superlattice	W	3	Cu	5	100	800
Copper Tungsten Superlattice	W	5	Cu	10	100	1500

Figure 9: The Superlattice samples which are available to be tested.

3.3 Oxide Sample Set

Another sample set was used in this project so as to provide context to the analysis of the superlattice data. The purpose of these samples was to study the interactions which occur within the samples which lead to a change in reflectance that is dependent on a change in temperature, and to investigate the EP coupling behavior of Indium Tin Oxide (ITO). ITO is a transparent conductive oxide, and is common in electro-optical applications. It exhibits a band gap which prevents it from interacting with light in the visible range. Due to its unique properties, developing successful methods of analysis could lead to extended thermal characterization capabilities in the future, for more complex systems.

The sample set itself is a combination of gold, titanium, and indium tin oxide in various arrangements. These samples are not superlattices and are mainly tested to work out kinks in the model and further gain some understanding of electron phonon coupling happening across layers. The details of the sample set are shown in Figure 10.

Sample Description	Layer 1	Thickness 1 (nm)	Layer 2	Thickness 2 (nm)	Layer 3	Thickness 3 (nm)
Gold thin layer	Au	5.3	---	---	---	---
Gold on ITO	Au	5.3	ITO	90	---	---
Gold Titanium Bilayer	Au	5.3	Ti	3	---	---
Gold Titanium Bilayer on ITO	Au	5.3	Ti	3	Indium Tin Oxide	90

Figure 10: The conductive oxide samples which are available to be tested.

4 Analytic Framework

Several different analytic frameworks were constructed and implemented to develop an understanding of the thermal transport that is happening inside the samples. Initially, a single layer model was used, where the whole sample was treated as a composite bulk sample. Two different thermoreflectance models were used in studying the signal based on this interpretation, a linear thermoreflectance model and a model which uses the Drude model to translate temperature to the dielectric function,[29] which is then used to model the reflectance of the sample.[13]

A multilayer model was then implemented, using the Crank Nicholson Method, to better determine the actual thermal transport which was occurring across layers and through the various interfaces in the samples. In this model the linear thermoreflectance model was not used, and the temperature dependent dielectric function model was combined with a graded multilayer optical model to get a thermoreflectance signal. These methods are all developed in the following sections, documenting much of the work done in this project.

4.1 Computational Implementation

In general, the method for understanding the thermal transport in these materials involves acquiring data through Time Domain Thermoreflectance, constructing a model which represents the physical system and its thermal evolution, and varying free parameters in order to solve for the properties of the system which we are studying.

In general, it is assumed that in the systems we are studying have some properties which

remain constant even when viewed at these time and length scales. These material properties are taken from literature and in some cases from bulk values to allow for a construction of a model which allows us to fit free parameters of interest and understand the system better.

In this study, the main parameter we are interested in is the electron phonon coupling factor (G). We propose that the effects of interfaces, mode restrictions, and various energy transfer pathways can be captured through this factor, which can generally show how electrons and phonons couple in the material. If this can indeed describe the way that materials react in a state of thermal electron phonon non-equilibrium, then it allows us to make assessments of how the various features of physical system in question affect the coupling we are interested in. There are other free parameters which were fit for over the course of the study, such as electron scattering rates and electron thermalization times, but these are not significantly complicating factors as they can be fit for in such a way that fitting one free parameter does not necessarily affect the fitting of another. For example, fitting the electron thermalization time can be done before electron phonon coupling really has a chance to occur, namely during the heating event, and so it can be fit over a different time scale, independently of the electron phonon coupling factor. This has to do with the sensitivity of the model to changes in properties across different time regimes of the signal. The varying sensitivity of the model to different properties across different time delay ranges make TDTR measurement very useful to work with due to the amount of information that can be gained from them.

4.2 One Dimensional Approximation

To start analyzing the system, it is necessary to understand the sensitivity of the model to some parameters which would otherwise complicate and encumber the modeling process. The most significant of these is the simplification of the model that can be made due to the organization and orientation of the pump pulse and the probe pulse of the TDTR system. Specifically, this simplification allows us to view the system in the frame of one dimensional heat transport.[30]

In TDTR, there are two pulses of light incident upon the sample for every heating event. One of these pulses is the pump, and the other is the probe. In our system, the pump pulse

has a wavelength of 404nm and generally operates with a diameter of about 50 μm. The probe pulse on the other hand has light with a wavelength of 808nm and has a diameter of about 12 μm. This difference in spot size is significant because it allows for a very useful simplification to the model.

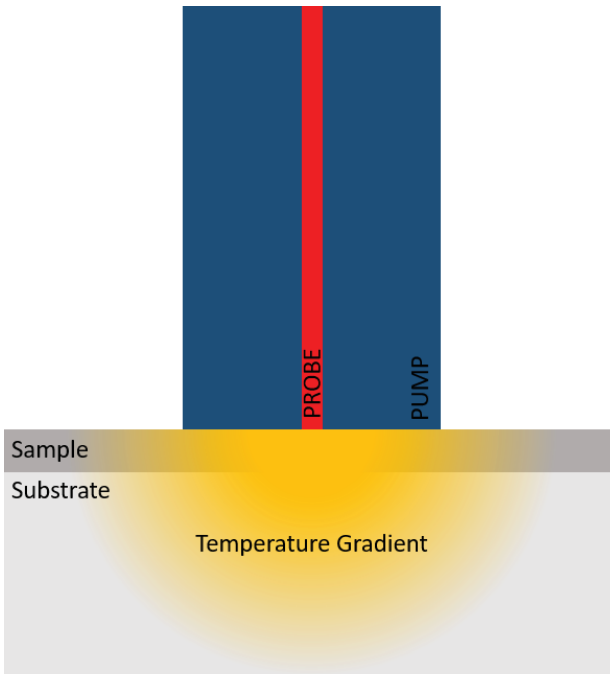

Figure 11: A cross sectional view of the relative beam sizes that allow for a one dimensional approximation.

With the heating event taking place over a relatively large area and with a generally Gaussian distribution of energy, there is a radial uniformity to the heating event which allows for the assumption that the spatial differential of the energy, and thus the temperature, is zero in the in-plane direction of the sample. In the area where the probe pulse hits the sample, the only significant thermal transport will will be normal to the surface of the sample because of this simplification. This allows for modeling the system in fairly understandable and computationally manageable ways, as opposed to the alternative, where a 3 dimensional model would need to be allowed to evolve in time, which is exponentially more computationally intensive and complex without gaining any accuracy. A cross section of the beam profiles can be seen in Figure 11, which gives an idea of the dimensionality we are interested in.

4.3 Single Layer Model

A single layer thermoreflectance model can be used to help in the understanding of thin film thermal transport and electron phonon coupling relative to other systems. This model involves just two temperature values at any individual time step, the electron temperature and phonon temperature of the thin film as a whole. This model primarily accounts for the initial coupling which occurs in the sample, and by design cannot capture any spatial effects which might be occurring due to diffusion in the material itself. The focus of fitting data using this model therefore is to understand on a basic level how different sample react in the non equilibrium state, and give insight into the differences in the relative behaviors of the materials. Comparison between different values produced by this model for different samples is what we are interested in for this analysis.

4.3.1 Thermal Model

In the single layer interpretation of the two temperature model as it relates to this system, we allow two individual temperatures to evolve in time, interacting through the TTM. By creating this interacting system in a fixed space, we can view how the energy appears to be transferred between the electrons and the phonons in the samples, introducing a source term allows us to properly model the energy input from the pump pulse of the TDTR setup. Using calibrated and well known laser parameters, we can model this impulse of energy accurately.

Some concessions need to be made in this model by trying to arrive at constants which are logical for the various thermophysical properties of the system. Weighted averages of the heat capacities and other constants were found to be the best representation of the systems, as they accounted for all the materials while maintaining a single layer context.

This single layer model allows for omitting spatial diffusion terms, allowing for a simple representation that shows how the system behaves relative to other systems, mainly as a function of varying electron phonon coupling in the system. A visual representation of this system of viewing the sample is shown in Figure 12

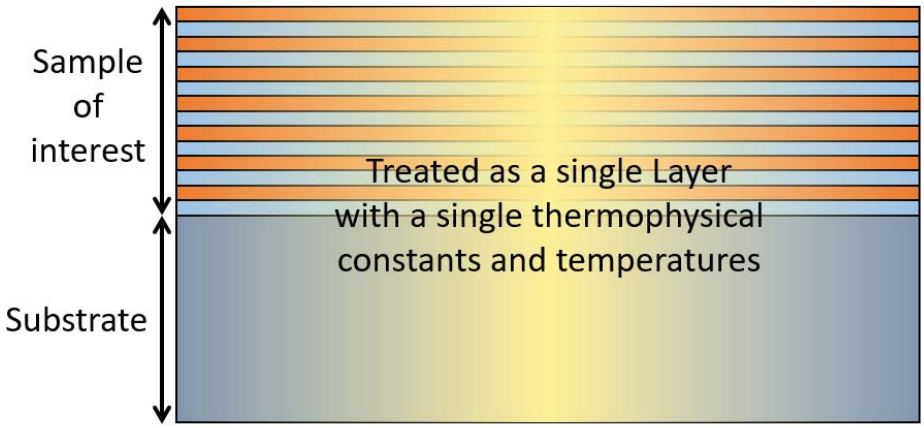

Figure 12: In the Single Composite Layer interpretation the whole sample is treated as a single thermal entity, subject only to a heating event and diffusion between the two temperatures in the TTM. This is shown with a representative superlattice sample.

4.3.2 Linear Thermoreflectance

One representation of thermoreflectance is the concept of a linear thermoreflectance model. This model operates through the following equation:

$$\Delta R = A \cdot \Delta T_e + B \cdot \Delta T_p \tag{4}$$

Upon first glance, this model may seem to be a not very rigorous approach to understanding thermoreflectance, but it has been shown that with small temperature changes ($< 150K$) this is indeed the tendency of the thermoreflectance signal.[21] More significant perhaps is that by understand how energy is added to the system in TDTR, this thermoreflectance representation does not require extensive knowledge of the electrodynamic properties of the materials in question.

Since the heating event is in this case a pulse of light, it is a reasonable assumption that the incident energy is initially deposited in the electrons. At the end of the heating event then, before any coupling between heat carriers occurs, the energy will solely be in the electrons of the system. Thus we are able to solve for A in the linear thermoreflectance model. At the peak of the thermoreflectance signal, we make the reasonable statement that $\Delta R(\Delta t = 0) = A \cdot \Delta T_e$ since $\Delta T_p = 0$. The change in thermoreflectance is known from the

data, and the change in temperature comes from the TTM.

This leaves only B as an unknown in the thermoreflectance model. An understanding of the time scales associated with electron phonon coupling allows us to get a grasp on the value of this constant as well. At 'large' times after the heating event ($t > 10ps$), we can reasonably assume that the electrons and the phonons have thermalized, and are at the same temperature. Thus $\Delta T_e = \Delta T_p = \Delta T$, and so $\Delta R = (A \cdot \Delta T)$. From this B can be solved for regardless of the rate that the energy coupled between the heat carriers, as it is the only unknown in the system at this time.

By allowing a single two temperature model to give us temperature as a function of time, we can then get a thermoreflectance signal as a function of the temperatures, and arrive at the end goal, a model where reflectance varies as a function of time. Using this model we can then vary the electron phonon coupling factor to fit to the tare at which the thermoreflectance signal decays to it's fully coupled value.

4.3.3 Dielectric Function Thermoreflectance

A more rigorous and potentially comprehensive model of thermoreflectance could come from the Drude model, where the material is treated as a free electron gas to allow for understanding the way that the electrons behave in the material, and the way they interact with light.[29]

The key to this model is that it directly relates the temperature to a thermoreflectance change without the need for any fitting in between. The first important equation in this model is the relationship between the electron collisional frequency and the electron and phonon temperatures:

$$\omega_\tau = A_{ee} T_e^2 + B_{ep} T_p \tag{5}$$

In this equation, ω_τ is the electron collisional frequency, A_{ee} is the electron electron scattering coefficient, and B_{ep} is the electron phonon scattering coefficient. This relationship is similar to the initial linear model we looked at previously, but uses scattering coefficients which can be solved for in other ways, making it useful for more complex systems.

From this electron collisional frequency, we can then extend this relationship to the dielectric function of the material:

$$\epsilon = 1 - \frac{\omega_p}{\omega - (\omega + i\omega_\tau)} \tag{6}$$

In this equation, ϵ is the dielectric function, ω_p is the plasma frequency of the material, ω is the frequency of the incident radiation, which is in this case the probe pulse, and finally ω_τ is the previously defined electron collisional frequency.

From this stage the dielectric function is then used to solve for the index of refraction (n) and the extinction coefficient (k) in the material for those temperatures, and those optical properties are used in a single thin film optical model to arrive at a thermoreflectance signal which can be fit to the acquired TDTR data.[13]

4.4 Multilayer Model

Due to the limitations of a single layer two temperature model there are certain phenomena in the data which cannot be accounted for with a single layer. Things which have a spatial dependence, such as back heating, depth dependent optical effects, interfacial transport rates, and interface reflectances can simply not be accounted for in a model which treats the system as a single layer. To address this and further our understanding of the thermal dynamics beyond relative electron phonon coupling rates, we need to understand the thermal transport through the system, spatially and temporally. This requires a more intensive numerical computation model and new considerations for the optical model used to represent the thermoreflectance.

4.4.1 Thermal Model

In the multilayer Two Temperature model, a nodal array of points is created that spans from the surface of the sample, through the sample and into the substrate. Each node has a defined temperature associated for the electrons and the phonons, a total energy that it holds, and a specific material that it is made up of which determines its specific thermal properties. This already sets a more rigorous standard than the single layer model in that

it allows us to account for the individual layers and their varied thermal transport rates.

Once representative nodal arrays for the material have been populated with known thermal properties, the next consideration is how to represent the heating event. We allowed for simple exponential decay of radiation intensity into the material, following established electrodynamics that allow for absorption of energy through the different layers.[31] The source term used properly accounts for the varied amounts of energy input by using established laser parameters and reflectance data for the pump pulse and gaussian time intensity profile for the pump pulse.

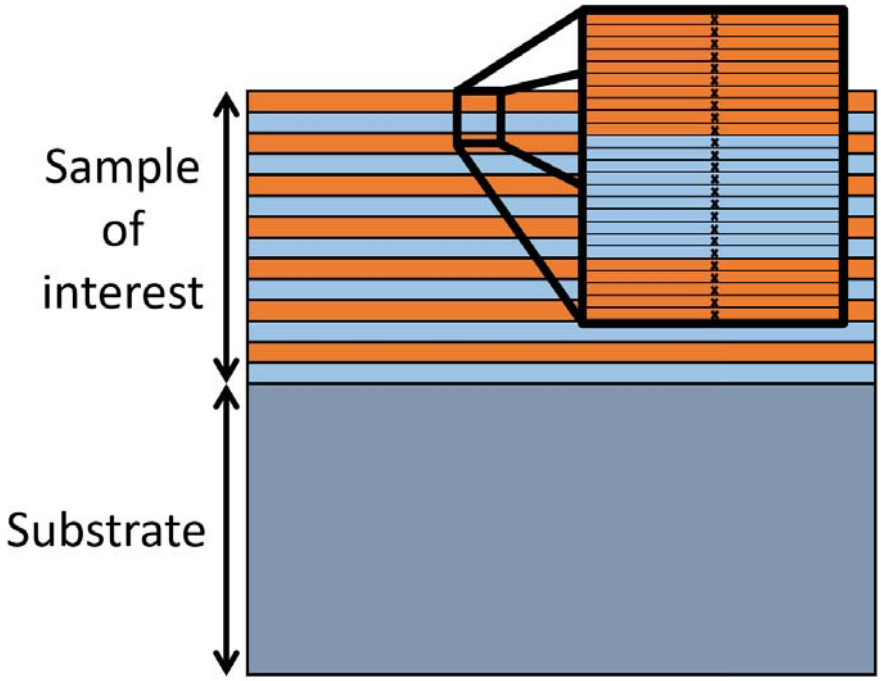

Figure 13: In the MultiLayer interpretation, the sample is broken up into one dimensional nodes which each have distinct temperatures in the TTM, and have the thermophysical properties of their respective materials. This is shown here with a representative superlattice sample. Each X in the figure is represented as a single node.

The biggest consideration with the multilayer thermal model is how to allow the energy to move through the system, and have the temperatures evolve with time. To achieve this we used a Crank Nicholson Differencing scheme which allows for good accuracy in the approximations made while maintaining an implicit framework. The biggest issue this model

solves is the matter of stability in such small time and length scales, where picoseconds and nanometers make a big difference. This model was implemented with every sample available, to give a proper treatment to the thermal phenomena which may spatially take place in the system being studied.[32] A visual representation of this method of interpreting the thermal system of the sample is shown in Figure 13.

4.4.2 Graded Multilayer Thermoreflectance

Along with this improved multilayer thermal model, there has to come a thermoreflectance representation which can take into account the level of complexity found in the system. This precludes us from using a linear thermoreflectance model in this case, as it generally only can take into account a single node, not an whole array of temperatures for the system. Extending it into a model that accounts for the spatial contributions is technically viable, but it is unclear what the actual mathematical method for such a model would be, and it is expected that it would not necessarily add accuracy compared to the model currently being used.

What we are left with then is the model for the dielectric function, which can, from the temperatures at each node, populate that node with an associated index of refraction and extinction coefficient, using the method described in Section 4.3.3.

The next step in this representation of the thermoreflectance comes from treating the complex index of refraction array as a graded multilayer system.[33] This manifests as an array of n values and k values. By taking each node's width and factoring in other physical parameters such as such as the wavelength of the light, we can utilize a thin film optical model to develop a thermoreflectance signal from the thermal model.

To start, we establish the electrical field equations which we will utilize:

$$E(x) = Re^{-ikx} + Le^{ikx} = A(x) + B(x) \tag{7}$$

E in this equation is the magnitude of the electric field, R is the amplitude of the wave traveling to the right, or through the film from the left, L is the amplitude of the wave traveling to the left, which is reflected, k is the wavenumber of the radiation, and A and B

are representative functions which represent the right moving and left moving parts of the electrical wave respectively.[**layered media**]

This equation helps us to relate the initial state of the electrical waves to end state through a matrix representation of the thin film system:

$$\begin{bmatrix} A_0 \\ B_0 \end{bmatrix} = \begin{bmatrix} M_{11} & M_{12} \\ M_{21} & M_{22} \end{bmatrix} \begin{bmatrix} A_s \\ B_s \end{bmatrix} \tag{8}$$

In this equation A and B are the right traveling and left traveling electric field intensities respectively, subscript 0 represents the free space region above the surface of the sample, subscript s is the substrate region, and M is the optical transfer matrix, with 4 respective elements.[33]

Equation (8) relates the incident intensities of electromagnetic radiation to the intensities in the substrate, past the system of interest. The next step is defining what the transfer matrix M actually is. This is established in the following equations, which combine propagation through the layer created at each node with the transitions between these nodal layers.

$$M = D_0^{-1}[\Pi_{l=1}^{N} D_l P_l D_l^{-1}] D_s \tag{9}$$

Where:

$$D_l = \begin{bmatrix} 1 & 1 \\ n_l & -n_l \end{bmatrix} \tag{10}$$

$$P_l = \begin{bmatrix} e^{-i\frac{2\pi n_l d}{\lambda}} & 0 \\ 0 & e^{i\frac{2\pi n_l d}{\lambda}} \end{bmatrix} \tag{11}$$

In the above equations, l denotes each layer, N is the total number of layers, D is the interface matrix, P is the propagation matrix, λ is the wavelength of the incident radiation, and M is the characteristic matrix of the system. Most importantly, n_l is the complex index of refraction for each nodal layer. The reflectance can be obtained from the resulting characteristic matrix by the following relationship:

$$R = |r|^2 = |\frac{M_{21}}{M_{11}}|^2 \tag{12}$$

This formulation allows us to establish the complex index of refraction through Drude Model Considerations, and then move the index of refraction into a spatially consistent thermoreflectance model. The end result is a situation where the reflectance is a function of all complex indices of refraction for each time step, and the complex index of refraction at each node is a function of the heat carrier temperatures at that node. This is a fairly robust and adaptable formulation of thermoreflectance which can be extended in the future as further study of how refractive indices can change with temperature is completed. Specifically, this model is fairly complete in that it can account for reflection that comes from gradients within layers, index changes across layers, and changes of the indices at the front and back nodes as well. This model presents a way to represent completely the optical features of the system, taking into account the entire system and any thermal diffusion which might occur, using the best interpretation currently available.

5 Results and Discussion

Several sets of conclusions, areas of discussion, and areas of future study arose from this project, with varying levels of applicability and implication for the transistor diffusion barriers, superlattice thermal diffusion, thermal and electronic transport through multilayers, and thermoreflectance. These results and other significant findings are discussed in this section.

5.1 Composite Single Layer Interpretation

As expected with a single layer view of the system, general trends were observed, but in such complex systems not all the dynamics were captured. The values produced in this analysis for the sample set are reported in Figure 14, with examples of data fits shown in Figure 15.

From these values it is clear that properties of superlattices are not just an average of the properties of the constituent materials. The values gathered for the effective electron phonon coupling factor in this interpretation are scattered, but generally consistent throughout the various data sets available for each sample. This indicates that there are interactions occurring between the electrons and the phonons throughout the multilayer system that are fundamentally different than if the individual elements were simply alloyed together. An

Sample Description	G (10^{16}W/m^{3}K)	$T_{e\text{-}e}$ (fs)
Cu Single Layer	6.96 +/- 5.1	370 +/- 60
Ta Single Layer	0.95 +/- 0.2	940 +/- 40
W Single Layer	7.22 +/- 0.2	290 +/- 10
5:5 Ta:Cu Superlattice	0.8 +/- 0.2	700 +/- 100
2:5 Ta:Cu Superlattice	0.86 +/- 0.2	960 +/- 30
5:10 Ta:Cu Superlattice	7.28 +/- 0.1	930 +/- 20
5:5 TaN:Cu Superlattice	0.97 +/- 0.3	930 +/- 50
2:5 TaN:Cu Superlattice	26.91 +/- 8.6	315 +/- 60
5:10 TaN:Cu Superlattice	4.53 +/- 0.1	460 +/- 80
5:5 W:Cu Superlattice	4.05 +/- 2.1	390 +/- 90
3:5 W:Cu Superlattice	4.49 +/- 0.1	260 +/- 30
5:10 W:Cu Superlattice	33.27 +/- 20.2	270 +/- 20

Figure 14: Resulting electron phonon coupling factors and electron electron thermalization times from using a composite single layer model.

easy example of this to look at is the difference between the copper and tungsten single layers and the copper tungsten superlattice results in Figure 14. Beyond this case, the superlattice electron phonon coupling factors are very varied, and do not seem to follow any simple trend in relation to the single layer values. This result lends validation to the merits of using a multilayer model as the dynamics occurring in the system might be more fully addressed with more avenues for energy transport. A note on the thermoreflectance model used: there were not significant difference shown between the dielectric function and linear thermoreflectance models using a single layer thermal diffusion model, and due to the lack of certainty regarding some electronic scattering parameters when viewing the superlattice as a composite single layer, the linear thermoreflectance model was dominantly used in this part of the study.

Beyond establishing some relative trends of the materials and superlattice data sets, the single layer model serves to highlight areas which are not capable of being addressed by the single layer model. Several phenomena inexplicable with a single layer diffusion model were observed, such as back heating, acoustic ringing, and extremely fast electron phonon coupling rates were observed which guided study going forward.

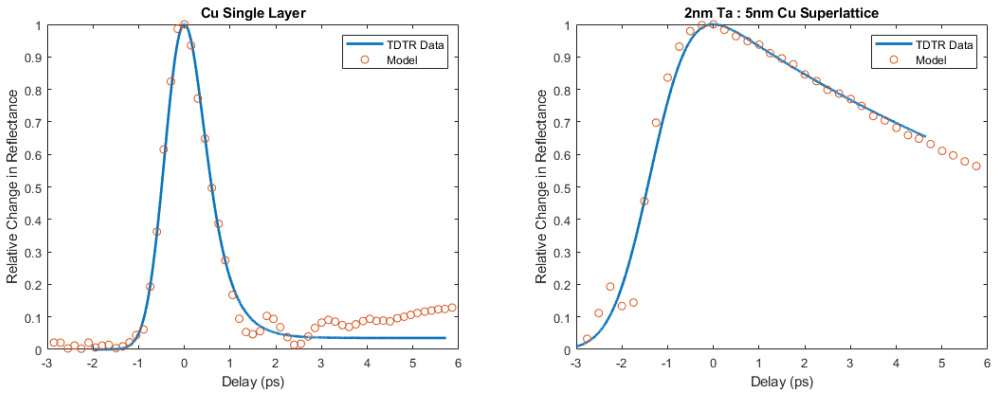

Figure 15: Graphs of data which show fits that the single layer model can interpret accurately.

5.2 Multilayer Interpretation

Upon developing the multilayer nodal thermal diffusion model and relating it to the data through the graded multilayer thermoreflectance model, we were able to fit and understand much more of the data accurately, establishing some useful conclusions about the nature of superlattices in the realm of electron phonon coupling.

The first product of this that we were able to draw was a relatively good agreement with literature values for the constituent components of the superlattice, as reported in Figure 16.

Material	G (10^{16}W/m^{3}K)	Literature Values
Cu	14.1 +/- 2.5	16.6 [1]
Ta	>1000	--
W	13 +/- 0.2	37.51 [1]

Figure 16: EP Coupling Factor results from a multilayer model.

This speaks to the validity of the methods we are using and ability of the model, within some reasonable error, to reproduce results which agree with reported literature values.

Beyond this agreement on single layer coupling factor values, we arrived at two other conclusions specific to electron phonon coupling in superlattices. First, we observed that when two materials which have very different electron phonon coupling factors are assembled in a superlattice, one material seems to dominate how the system behaves as a whole than the other. This can be seen significantly in Figures 17 and 18, where the electron phonon

coupling factor of copper seems to be influenced by the very fast electron phonon coupling which seems to be happening in Tantalum. This coupling between the two properties of the materials could be caused by the cohesive nature of the interfaces which connect the layers of the superlattice, but this is not explicitly clear based on available data.

Material	G (10^{16}W/m^{3}K)
Cu	14.1 +/- 2.5
Ta	>1000

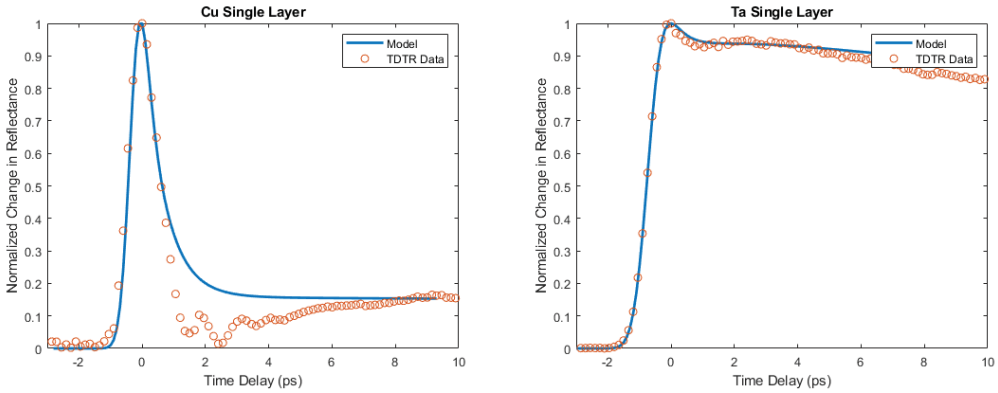

Figure 17: Thermal behavior in single layers, to be contrasted with the behaviors seen in superlattices of the same materials in Figure 18.

The second significant conclusion to be made about superlattice electron phonon coupling is that the layer thickness of the individual layers plays a significant role in the response to the heating event. This difference could be due to the restricted phonon modes, increased spatial frequency of interfaces, defects which only occur at thinner layer thicknesses, or varied thermoreflectance contributions. The general trend, however, appears to be that as the layers become thinner and the periodic structure repeats more frequently, the electron phonon coupling occurs at a faster rate. This is an interesting result, which runs slightly contrary to expectations, as electrons should be able to move very coherently across the superlattice boundaries, as well as phonons, so increased layer frequency should not theoretically play a significant role. This difference in apparent behavior can be seen in Figures 19 and 20.

Material	G (10^{16}W/m^{3}K)
Cu	199 +/- 56
Ta	>1000

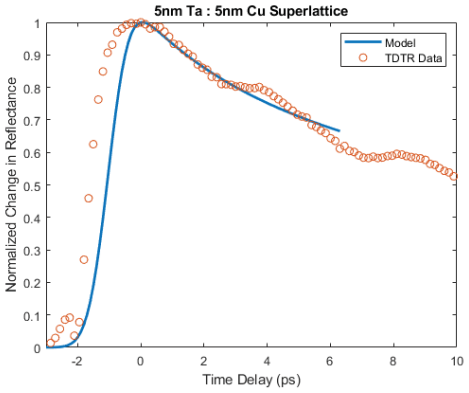

Figure 18: Thermal behavior in single layers, to be contrasted with the behaviors seen in single layers of the same materials in Figure 17.

Material	G (10^{16}W/m^{3}K)	Layer Thickness
Cu	200 +/- 42	5nm
TaN	>1000	5nm

Material	G (10^{16}W/m^{3}K)	Layer Thickness
Cu	15 +/- 3	5nm
TaN	120 +/- 5	10nm

Figure 19: Determined values for different layer thicknesses of a type of superlattice.

5.3 Electron Thermalization Time

We did not only study EP coupling factors in this project. Bundled in with the increased understanding of this property in these systems comes a greater understanding of the electron thermalization behaviors in superlattices. This can be most easily thought of as the time it takes for electrons which have been excited by incident photons in the pump pulse to actually contribute to the statistical mechanical temperature of the electron population. This electron thermalization time affects the actual thermal model used by altering to the formulation of the source term used, and experiences significant variation in different superlattice configurations. There is no a easily discernable trend of dependence of the thermalization time due to the limits of the samples available at different layer thicknesses, but what can

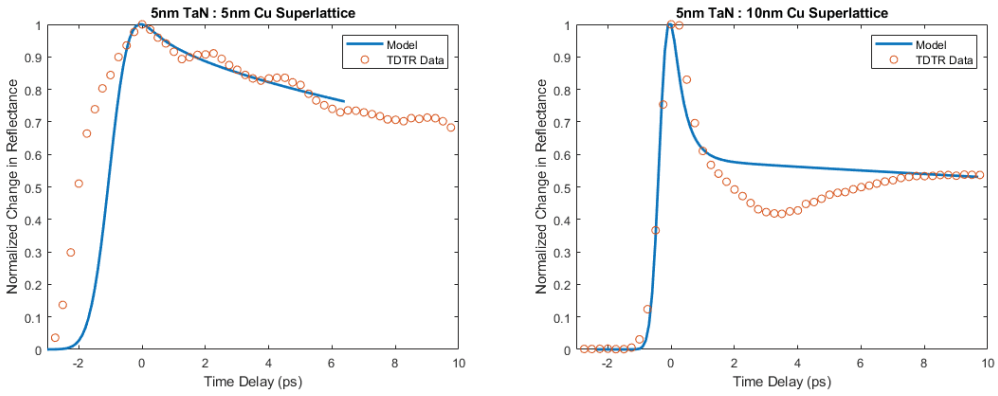

Figure 20: Data representations of the results from Figure 19. Notably the TDTR responses to the different layer thicknesses even show significant change.

be seen is a similar effect based on the relative layer thicknesses, where the longest electron thermalization time seems to occur when the superlattice has even thickness layers of alternating materials. This trend is represented in the numbers reported in Figure 14, and is shown graphically in Figure 21.

This speaks to the rate and correspondingly probability in time that an energetic electron will thermalize in these systems. This seems to have a good analog in its use as a diffusion barrier in transistors, as it indicates that a superlattice with even alternating layer thicknesses will allow more energetic electrons to exist outside the general electron population state for a longer period of time.

The reason for this difference in thermalization time with different layer thicknesses is not immediately evident, but seems to be caused by the irregularity in spatial frequency of the interfaces that the electrons encounter. It is possible that the combination of ideal layer thickness and regular interfaces allows thermalization time to reach a peak at the 5nm : 5nm superlattice due to a balance of layer thickness which is small enough to minimize coupling in a layer before transition to another layer, but large enough to not have too many interfaces to cross close to the surface of the sample. This requires further investigation for a more complete explanation however.

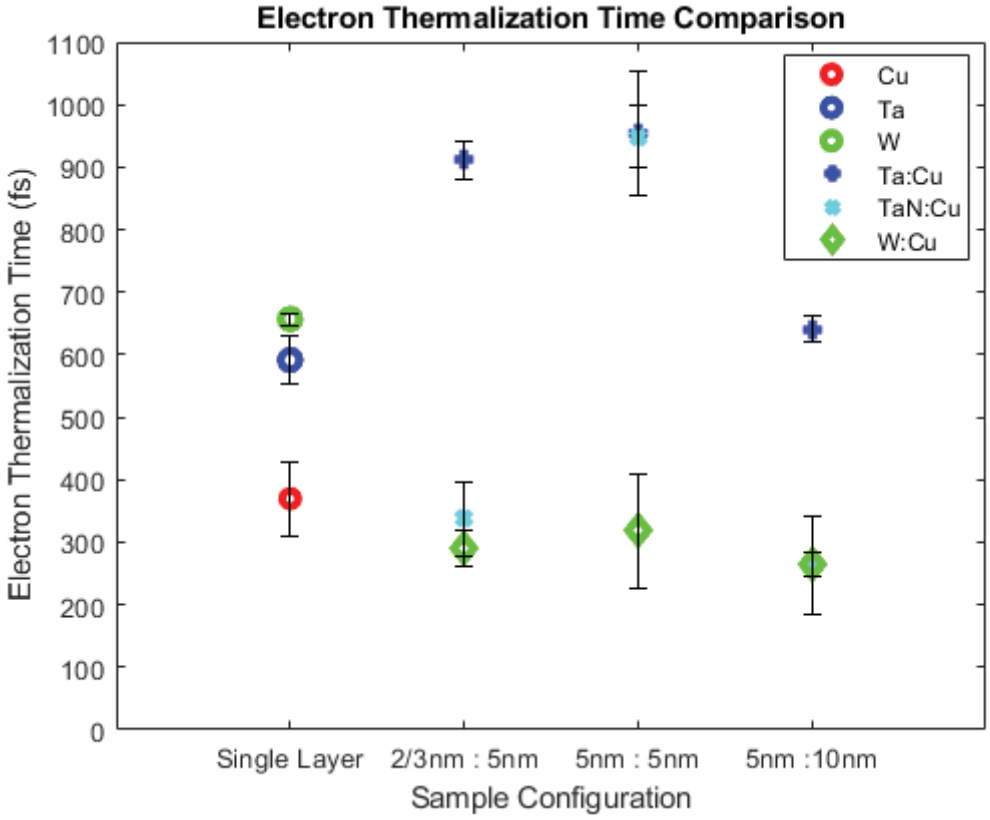

Figure 21: Depiction of the Dependence of thermalization time on various superlattice layer configurations.

5.4 Progression of Testing on the Oxide Sample Set

The Oxide sample set in this project represents an attempt to extend our fundamental understanding of thermoreflectance and further validate the completeness and adaptability of the thermal model by studying a slightly less complex system. With only 4 samples to consider, a progression of testing and analysis was developed which would allow for the fitting of electron phonon coupling in some materials that would not otherwise lend themselves to this sort of testing.

Through progressively increasing the complexity of the system analyzed, properties of various parts of the system can be confidently determined. By starting with a gold single layer, adding a layer of titanium, and then adding a layer of ITO, we can fill in the lack of understanding we have about the system progressively, with each iteration adding complexity

and understanding.

With this specific data set we first analyze the gold single layer using our complete multilayer thermal model and graded multilayer thermoreflectance model. This results in very comfortable fitting of the data and confirmation of the scattering parameters of the single layer, as seen in Figure 22.

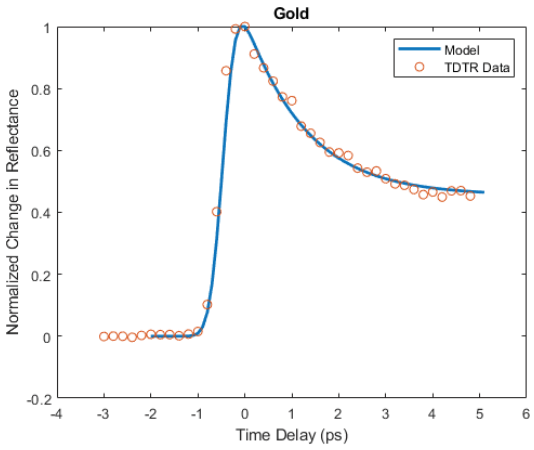

Figure 22: A fit of Gold, with a value of G of 2.4 +/- 0.2, in excellent agreement with reported values.[13]

Adding complexity to this system, we then test the Gold and Titanium bilayer, and fit for scattering coefficients in titanium using an expected Titanium electron phonon coupling range of between 2e17 $\frac{W}{m^3K}$ and 2e18 $\frac{W}{m^3K}$.[23] While this fit fairly well, it did deviate from the model slightly, as shown in Figure 23. The deviation in this case seems to be from an energy sink which is not being accounted for. The specific issue which is affecting the fit in this case is that using established methods of calculating thermoreflectance and using heat capacities and thermophysical properties determined for tungsten, too much energy is trapped in the electrons of the Titanium layer, and is transferred back into the gold layer which then affects the thermoreflectance.

In the next sample considered, a thick (90nm) layer of ITO was added in between the insulating glass. In this sample, energy can be transferred out of the Titanium layer at a much higher rate, allowing for the proper fitting of the data, as seen in Figure 24. This good representation uses the values calculated in the previous two calculations to account

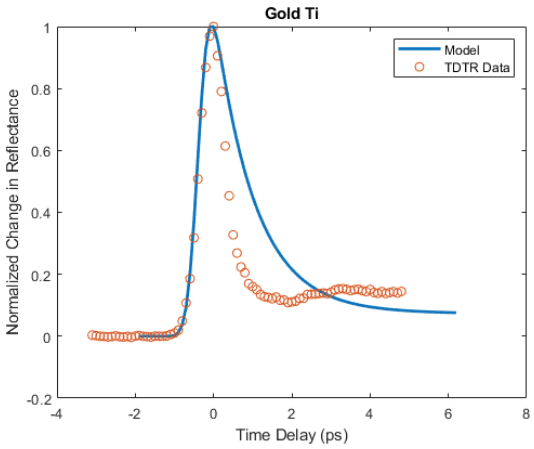

Figure 23: Gold Titanium Bilayer fitting, showing some deviation but still representing the trends expected.

for thermal diffusion in the system.

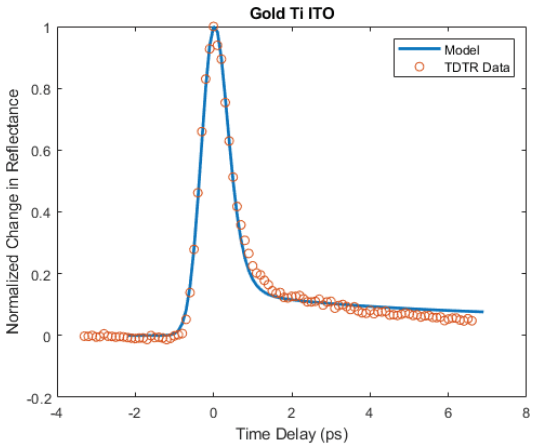

Figure 24: Gold Titanium Bilayer on ITO fitting. As can be seen qualitatively, the addition of a the Indium Tin Oxide significantly helped our ability to fit the data to our model.

This leads to reasonable values of the electron phonon coupling factors in the system, which are reported in Figure 25. These values follow logically from reported literature values and extend the understanding of Indium Tin Oxide's thermal properties.

Material	G (10^{16}W/m^{3}K)
Au	2.4 +/- 0.2
Ti	18 +/- 0.29
ITO	120 +/- 34

Figure 25: Numerical results of the Oxide data set fitting.

5.5 Electron and Phonon Heat sinks

A specific area of consideration which played a significant part in the understanding of most of these systems is the idea of electron and phonon heat sinks. Put another way, we need to consider that energy can become trapped in a certain location within the system, and then redistributed through a different transfer mechanism than that through which it arrived. This phenomenon can be seen very clearly in both the superlattice data sets and the oxide data sets.

The most evident way that this occurs is what is known as back heating, where energy enters the system in a layer away from the surface in the electrons, couples into the phonons of that layer, and then is transferred through the interface to back to the first layer. Since most of the thermoreflectance contribution comes from the first layer based on the penetration depths of the wavelengths of light used, the signal responds to this heating by driving the signal up a few picoseconds after the initial heating event. This heat transfer is depicted in some of the data sets, and shows a complicating factor which is not always simple to fit to, especially in the superlattice samples. It is assumed in the superlattice structures that each layer will have the same properties as the other layers of the same material in the sample. Because of this idea, accounting for back heating can cause complications to the rest of the fit in the sample which has many periodic layers.

This back and forth transfer of energy ends up complicating the interpretation of many of the data sets, and can have a significant impact on the thermoreflectance signal over time. As energy gets trapped and sent back towards the surface of the sample, it will confuse the normal energy transfer and thermal transport which is occurring near the surface in the top

layer of the material, and cause complications with fitting the data and understanding the story behind the data. Some examples of back heating are shown in Figure 26.

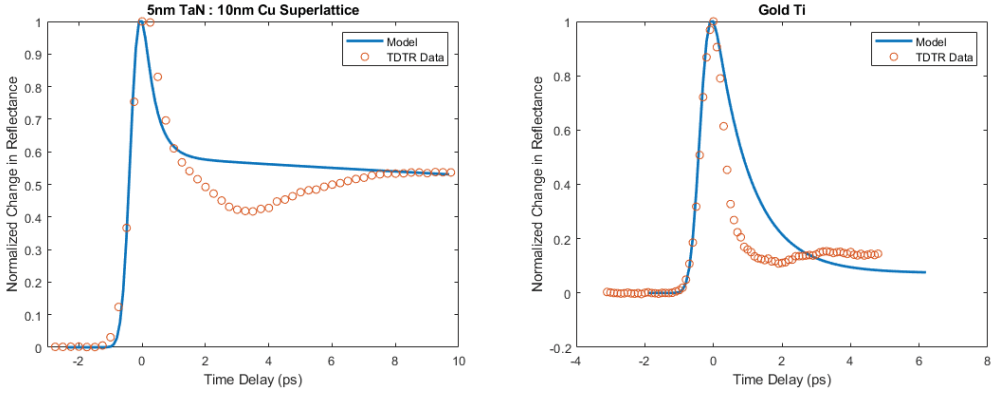

Figure 26: Examples of data-model deviations which could be caused by back heating, among other considerations.

Back heating does not necessarily fully explain the phenomenon of a rise after an initial local minimum in the signal after the heating event however. Another possible factor can be found in the concept of strain.

5.6 Strain Waves

Strain waves affect much of the TDTR data gathered in some way or another. They are essentially sound waves which move from the heating event into the sample, carrying a small amount of energy as they go. Strain waves are energetic waves that can be best thought of as a wave that is generated during the heating event, and moves through the material causing the atoms in the material to subtly swell as it passes. This swell is understood to affect the thermoreflectance in a way that is not very well accounted for in the thermoreflectance model which was implemented in this project.[21] The strain in the sample is then an aspect of the thermal transport in the material which complicates the data seen.

Strain can have several effects on TDTR data. The first and most easily understood effect is an oscillatory signal which appears as the wave propagates through the sample, reflecting off of regularly spaced interfaces and causing a ringing to be seen in the data as the strain wave arrives back at the surface of the sample. The strain is then reflected

again and the oscillations that are seen are produced. This is clearly shown in Figure 27. It does not make the data necessarily more difficult to fit, as it manifests as an overlaid sine wave a few picoseconds into the data. As such it was not a particular issue which needed to be addressed in the study. Notably, this effect only occurs in superlattices where the ratio of layer thicknesses of the materials is the same, supporting our interpretation of this phenomenon in the data, as evenly spaced layers will lead to compounding of reflections and the oscillatory signal we observe.

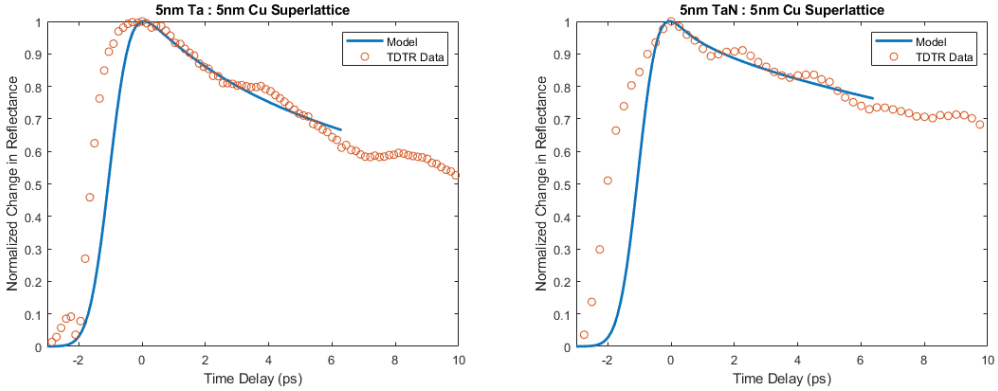

Figure 27: Strain Wave oscillation examples.

In other samples, where reflections cannot be compounded by regular layer thicknesses, the effect of strain is less clear. In some cases, where the back heating model cannot necessarily account for a dip in the signal, strain may be the cause. A wave which moves away from the surface through the sample could logically contribute to some of the deviations in the data seen, particularly in the data sets where back heating was a significant consideration, shown in Figure 26. It appears that a combination of many small factors combine to make the data more difficult to interpret for some samples, and while others are clean and easier to comprehend, others are more unsure due to the complications. The current formulation of the model as a whole does not take into account strain waves, adding a little uncertainty to some of the data points in the experiment.

5.7 Thermoreflectance

This whole study is predicated on the notion that a change in the temperatures of the electrons and phonons in a system can change the reflectance signal seen in TDTR. This is an incredibly powerful idea that has been experimentally and theoretically flushed out in many areas, through accurate and consistent modeling of observed thermal behaviors.[16, 34, 13, 35] We reproduce these results in Figure 22, where it is clear that the model is accurately fitting to the data. We developed our own method for modeling the thermoreflectance in this study, and it is based on the idea that the material being tested behaves as described by a free electron model, and that the index of refraction and extinction coefficient can give a complete description of reflectance behaviors. For materials such as Gold, and to a slightly lesser extent, Copper, this assumption is quite valid and yields results which speak to the validity of the model.[16, 36]

This is the reason that in many other thermal measurements made with TDTR, a transducer layer is used where the thermoreflectance response is known to a higher degree for that material.[37] Using an optical transducer in TDTR however precludes the study of Electron Phonon coupling in the material. The reason for this is that with a transducer of necessary thickness to isolate the thermoreflectance signal, the response to electron phonon coupling beyond the transducer layer is dampened to a degree that the a model used would no longer be sensitive enough to changes in it to be very useful.

In this study then, no transducer layer was present on the superlattices, and the radiation was incident directly on the sample of interest. The issue then becomes how to interpret the modeled heat diffusion as a change in thermoreflectance. The most robust method available that gives dependence on both the electron and phonon temperatures of the material is the Drude Model, which is a free electron model, which as previously discussed accounts for the electron and phonon temperatures in its formulation through the effects on electron scattering rates. The materials being placed in superlattices however do not behave exactly as free electron gasses, as their respective band structures, observed TDTR response, and resistivities show. The Drude model did produce the best possible representation of the data for this project however, as no better model for this specific physical phenomenon is

currently developed.[38, 20, 39]

One new progression in this project has been the establishment of a graded multilayer model which uses the complex index of refraction in a nodal array to produce a thermoreflectance change. This model is the most physically accurate we encountered and simplifies the question of thermoreflectance significantly, making the question more to do with how the temperatures within the sample affect the index of refraction instead of a direct translation to reflectance. This simplification may be significant in understanding thermoreflectance going forward.[39, 38] There are however more complications to be considered beyond this, specifically focused on two aspects of multilayer systems, band structures of the materials and interfacial contributions to the thermoreflectance.

Band structures give an idea of the energy transitions which are allowed within a material. The current model which we use for thermoreflectance restricts the transitions to intraband transitions, essentially allowing energy transitions which don't require jumps across band gaps.[40, 13, 23] This is a valid assumption for a good number of the materials used, specifically due to the probe wavelength used of 808 nm. This is for the most part not enough energy per photon to create interband transitions in the materials we care about, and so the model retains accuracy. In some materials however, this is not the case. The temperature dependence contributions that interband transitions add to the change in the complex refractive index, and by extension the reflectance, are not clear. [13]

Interfaces add an additional level of complexity which is difficult to understand fully. With each interface, there will be reflection due to a discontinuous change in the refractive index of the material. Since many of the interfaces in our samples are located in the sample well within the skin depth of the probe beam, the contributions they have cannot be discounted. We can account for a change in index in the Graded Multilayer Model totally fine, as the nodal model can handle discontinuities by nature of using discrete values of n and k at each node. However, certain aspects of the data show that even given this understanding of the index representation of thermoreflectance, there may be contributions which we are not accounting for. Looking specifically at the oxide multilayers, shown in Figure 28, the issue becomes more apparent.

The specific issue which we encounter that our current thermoreflectance model cannot

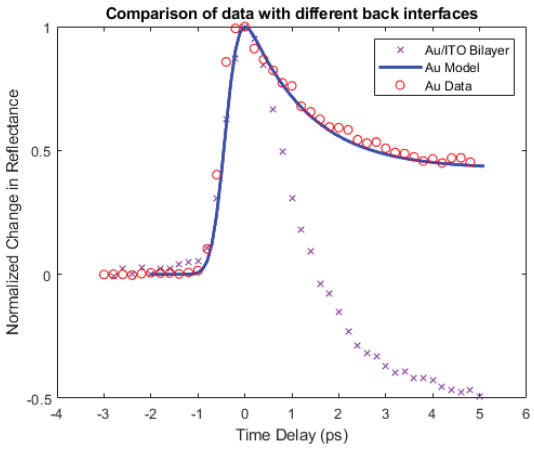

Figure 28: A comparison of Au/glass (red) and Au/ITO/glass (purple) which highlights the issues that can arise from interfaces. In this specific sample the thermoreflectance signal hits a peak and then crosses the zero point. This is an area which needs further development.

account for is the drop of the thermoreflectance signal below its initial value after reaching an initial peak. With the Drude model based thermoreflectance, the only change in thermoreflectance that can be produced will be in the same direction for a single heating event. This crossing zero behavior can be accounted for using a linear thermoreflectance model, but using that workaround fundamentally ignores the physics which is happening in this specific instance, and isn't applicable to multilayer models, as previously discussed.

The complexity of the issue is highlighted by considering the exact geometry of the samples in Figure 28. The metal layer in the samples is identical, with the only difference being a layer of ITO behind the Gold in the bilayer sample. ITO is a transparent conductive oxide, so it is expected that it will not significantly interact optically with the probe pulse compared to the gold layer. Using this assumption, the only functional difference between the two samples is the electrical conductivity of the back interface of the gold. The change in reflectance over longer times seems to then be an effect of the conductivity of this interface. As energy moves to the interface from the surface, the signal is driven down below its initial value. This same behavior however is not seen in the Gold Titanium sample on the ITO, which throws into question why the Gold ITO interface is having such a drastic effect on the TDTR signal, as it doesn't seem to just have to do with the conductivity. There is not a good answer to the question of why there is this change in behavior over time for that specific

sample, but being able to answer it may allow for accounting for TDTR data irregularities to a degree which was not possible to this point.[22] It is worth noting that this TDTR signal artifact of crossing zero after the heating event was also observed in all of the superlattices of Tungsten, which made the EP coupling factors for Tungsten difficult to interpret. Potential explanations are that competing thermoreflectance signals are being produced by different parts of the sample, and as energy moves through these parts, different thermoreflectance signals are made more and less prominent. Working toward a comprehensive model which can account for these deviations, and the specific effects of interfaces on thermoreflectance is an endeavor worth pursuing.

The whole idea of thermoreflectance, while powerful, is fickle in what it gives based on the specific sample it is being used to study. The establishment of a more robust and fundamentally accurate thermoreflectance model is a topic which should be pursued to further the applicability of TDTR as a thermal characterization method.

6 Conclusions

In this study we approached two sample sets from an experimental perspective and attempted to deepen our understanding of the thermal characteristics of the physical systems through time domain thermoreflectance measurements and modeling the system and heating event. We were overall able to arrive at some useful conclusions regarding the thermal properties of these systems.

6.1 Superlattice Dynamics

Within the superlattices tested, certain trends in the data were observed. To start, EP Coupling factors in the materials were reported as very different in single layers than they were in superlattices. The extreme thinness of the layers and the coherence with which they are bonded allows the EP coupling factors to interact so that the behaviors of EP coupling within the layers are themselves coupled together. This could be due to carrier coupling across material boundaries, interactions of the energetic structures of the materials, or phonon mode restrictions. In any case, the change in the EP Coupling factors was such

that the representative material values moved closer together in cases where the materials were placed in superlattices.

The EP coupling within superlattices of different layer thicknesses was also found to vary greatly based on the layer thicknesses that were used. For each superlattice configuration, a fairly unique signal was produced, which fit EP Coupling factors very differently for different configurations of the same material. In general, superlattices with relatively thick layers seemed to fit to lower EP coupling factors. This is thought to be due to the ability for the layers to behave more as they would in bulk materials, and thus couple less with each other through the boundaries of the materials.

This all leads to some useful outcomes for the stated goal of this project, which was to provide some observations on the physics occurring in these samples. In general, it appears that using uniform layer thicknesses throughout in a superlattice with relatively thick layers is the best solution to provide a diffusion barrier for use in microelectronic design, while maintaining the desired properties. These superlattices can lower the limiting factor of coupling in a single layer system by dragging down the highest EP coupling factor found in the system. This configuration would potentially allow for the weakest overall electron phonon coupling behavior through the diffusion barrier, which would allow for less cumulative resistance in the flow of energy through the barrier, and minimized thermal buildup. This is further supported by observations of electron thermalization time, which shows a trend of allowing slower energy transfer between populations of heat carriers in the even multilayer superlattices. This should be tested further as to the optimized layer thicknesses within the system, but these conclusions could be used as guiding figures in improving microelectronic design.

6.2 Conductive Oxide Properties

In the samples tested in pursuit of determining the electron phonon coupling behavior of Indium Tin Oxide, we were able to fit the model developed to study the superlattice systems to a simpler multilayer system and determine a reasonable value of electron phonon coupling in ITO. The reported values in Figure 25 represent a step forward in understanding these materials.

6.3 Thermoreflectance

As discussed in section 5.7, advances to the interpretation of thermoreflectance were made in the implementation of a nodal multilayer model which used Drude model interpretations of the effect of temperature on the complex index of refraction of the material to produce a thermoreflectance signal. Several areas of further study were identified and observations were made regarding the role of interfaces in affecting the thermoreflectance of a system.

6.4 Nanoscale Thermal Diffusion Modeling Developments

In general a methodology for understanding nanoscale thermal diffusion in complex systems was developed and utilized, and certain thermal phenomena, such as electron phonon coupling, back heating, strain, interfacial effects, and scattering rate considerations were studied for various materials and systems to develop a deeper understanding of nanoscale thermal and electronic transport. This methodology will be useful in studying further complex nanoscale systems, and with additional development of the thermoreflectance models used, could give an extremely adaptable and far reaching tool for the study of the thermal properties of extensive nanoscale systems.

References

[1] Robert R. Schaller. "Moore's Law: past , present , future". In: *IEEE spectrum* 34.6 (1997), pp. 52–59. ISSN: 0018-9235. DOI: 10.1109/6.591665.

[2] Scott E. Thompson and Srivatsan Parthasarathy. "Moore's law: the future of Si microelectronics". In: *Materials Today* 9.6 (2006), pp. 20–25. ISSN: 13697021. DOI: 10.1016/S1369-7021(06)71539-5.

[3] Eric Pop. "Energy dissipation and transport in nanoscale devices". In: *Nano Research* 3.3 (2010), pp. 147–169. ISSN: 19980124. DOI: 10.1007/s12274-010-1019-z. arXiv: 1003.4058.

[4] John Loeffler. *No More Transistors: The End of Moore's Law*. 2018. URL: https://interestingengineering.com/no-more-transistors-the-end-of-moores-law.

[5] L.S. "The End of Moore's Law". In: *The Economist* (2015). URL: https://www.economist.com/the-economist-explains/2015/04/19/the-end-of-moores-law.

[6] a Majumdar, K Fushinobu, and K Hijikata. "Effect of gate voltage on hot-electron and hot-phonon interaction and transport in a submicronmeter transistor". In: *Journal of Applied Physics* 77.12 (1995).

[7] Eric Pop et al. "Localized heating effects and scaling of sub-0.18 micron CMOS devices". In: *Technical Digest-International Electron Devices Meeting* (2001), pp. 677–680. ISSN: 01631918. DOI: 10.1109/IEDM.2001.979598.

[8] Karen Holloway et al. "Tantalum as a diffusion barrier between copper and silicon: Failure mechanism and effect of nitrogen additions". In: *Journal of Applied Physics* 71.11 (1992), pp. 5433–5444. ISSN: 00218979. DOI: 10.1063/1.350566.

[9] Tomi Laurila et al. "Failure mechanism of Ta diffusion barrier between Cu and Si". In: *Journal of Applied Physics* 88.3377 (2000). DOI: 10.1063/1.1288692.

[10] Yoon-jik Lee et al. "Barrier properties and failure mechanism of Ta – Si – N thin films for Cu interconnection". In: *Journal of Applied Physics* 1927.1999 (1999). DOI: 10.1063/1.369172.

[11] Kow Ming Chang et al. "Amorphouslike chemical vapor deposited tungsten diffusion barrier for copper metallization and effects of nitrogen addition". In: *Journal of Applied Physics* 82.3 (1997), pp. 1469–1475. ISSN: 00218979. DOI: 10.1063/1.365925.

[12] M. H. Tsai et al. "Comparison of the diffusion barrier properties of chemical-vapor-deposited TaN and sputtered TaN between Cu and Si". In: *Journal of Applied Physics* 79.9 (1996), pp. 6932–6938. ISSN: 00218979. DOI: 10.1063/1.361518.

[13] Ashutosh Giri. "The role of electronic and vibrational scattering on thermal transport across multiple interfaces in nanostructures". PhD thesis. University of Virginia, 2016.

[14] Eric Pop, Sanjiv Sinha, and Kenneth E. Goodson. "Heat generation and transport in nanometer-scale transistors". In: *Proceedings of the IEEE* 94.8 (2006), pp. 1587–1601. ISSN: 00189219. DOI: 10.1109/JPROC.2006.879794.

[15] Daniel Schroeder. *An Introduction to Thermal Physics*. 1st ed. Robin J Heyden, 2000. ISBN: 0-201-38027-7.

[16] Patrick E. Hopkins et al. "Ultrafast and steady-state laser heating effects on electron relaxation and phonon coupling mechanisms in thin gold films". In: *Applied Physics Letters* 103.211910 (2013). ISSN: 00036951. DOI: 10.1063/1.4833415.

[17] David G. Cahill et al. "Nanoscale thermal transport". In: *Journal of Applied Physics* 93.793 (2003), pp. 793–818. ISSN: 00218979. DOI: 10.1063/1.1524305. arXiv: 1609.08133.

[18] R. B. Wilson et al. "Two-channel model for nonequilibrium thermal transport in pump-probe experiments". In: *Physical Review B - Condensed Matter and Materials Physics* 88.14 (2013), pp. 1–11. ISSN: 10980121. DOI: 10.1103/PhysRevB.88.144305.

[19] David Griffiths. *Introduction to Quantum Mechanics*. 2nd ed. Prentice Hall, 2005. ISBN: 0-13-111892-7.

[20] William J. Topf, Michael E. Thomas, and Terry J. Harris. "Optical and Physical Properties of Materials Crystals and Glasses". In: *Optical and Physical Properties of Materials*. 1995. Chap. 33, pp. 33.1–33.101.

[21] Pamela M. Norris et al. “Femtosecond pump–probe nondestructive examination of materials”. In: *Review of Scientific Instruments* 74.1 (2003), pp. 400–406. ISSN: 0034-6748. DOI: 10.1063/1.1517187.

[22] Y. Wang et al. “Effect of interlayer on the interfacial thermal transport and hot electron cooling in metal-dielectric system: An electron-phonon perspective”. In: *Journal of Applied Physics* 119.065103 (2016).

[23] Zhibin Lin, Leonid V. Zhigilei, and Vittorio Celli. “Electron-phonon coupling and electron heat capacity of metals under conditions of strong electron-phonon nonequilibrium”. In: *Physical Review B - Condensed Matter and Materials Physics* 77.7 (2008), pp. 1–17. ISSN: 10980121. DOI: 10.1103/PhysRevB.77.075133.

[24] Elah Bozorg-Grayeli et al. “High temperature thermal properties of thin tantalum nitride films”. In: *Applied Physics Letters* 99.261906 (2011), pp. 1–4. ISSN: 00036951. DOI: 10.1063/1.3672098.

[25] J. H. Weaver, C. G. Olson, and D. W. Lynch. “Optical properties of crystalline tungsten”. In: *Physical Review B* 12.4 (1975), pp. 1293–1297.

[26] David G. Cahill et al. “Nanoscale thermal transport. II. 2003-2012”. In: *Applied Physics Reviews* 1.011305 (2014). ISSN: 19319401. DOI: 10.1063/1.4832615.

[27] Jeppe Byskov-Nielsen et al. “Ultra-short pulse laser ablation of copper, silver and tungsten: Experimental data and two-temperature model simulations”. In: *Applied Physics A: Materials Science and Processing* 103.2 (2011), pp. 447–453. ISSN: 09478396. DOI: 10.1007/s00339-011-6363-7. URL: http://link.springer.com/10.1007/s00339-011-6363-7.

[28] Ashutosh Giri et al. “Mechanisms of nonequilibrium electron-phonon coupling and thermal conductance at interfaces”. In: *Journal of Applied Physics* 117.10 (2015). ISSN: 10897550. DOI: 10.1063/1.4914867.

[29] Mihailo Markovic and Aleksandar D Rakic. “Determination of the reflection coefficients of laser light of wavelengths (0.22 um, 200 um)from the surface of aluminum useing the lorentz drude model”. In: *Applied Optics* February 1989 (1990), pp. 1–5.

[30] Patrick E. Hopkins et al. “Criteria for Cross-Plane Dominated Thermal Transport in Multilayer Thin Film Systems During Modulated Laser Heating”. In: *Journal of Heat Transfer* 132.8 (2010), p. 081302. ISSN: 00221481. DOI: 10.1115/1.4000993. URL: http://heattransfer.asmedigitalcollection.asme.org/article.aspx?articleid=1449217.

[31] Eugene Hecht. *Optics*. 4th ed. San Francisco: Pearson Education, 2002. ISBN: 0-8053-8566-5.

[32] G Chen. “Thermal Conductivity and Ballistic Phonon Transport in Cross-PlaneDirection of Superlattices”. In: *Physical Review B* 57.23 (1998), pp. 14958–14973. URL: z:%7B%5C%%7D5CArticles%7B%5C%%7D5Csuperlattices-perpendicular%7B%5C%%7D5CChen-PRB-1998.pdf.

[33] Pochi Yeh. *Optical Waves in Layered Media*. 1988. ISBN: 0-471-82866-1.

[34] S. D. Brorson et al. “Femtosecond room-temperature measurement of the electron-phonon coupling constant in metallic superconductors”. In: *Physical Review Letters* 64.18 (1990), pp. 2172–2175. ISSN: 00319007. DOI: 10.1103/PhysRevLett.64.2172.

[35] Hai Dong Wang et al. “Measurements of electron - Phonon coupling factor and interfacial thermal resistance of metallic nano-films using a transient thermoreflectance technique”. In: *Chinese Physics B* 20.4 (2011). ISSN: 16741056. DOI: 10.1088/1674-1056/20/4/040701.

[36] H. E. Elsayed-Ali et al. “Time-resolved observation of electron-phonon relaxation in copper”. In: *Physical Review Letters* 58.12 (1987), pp. 1212–1215. ISSN: 00319007. DOI: 10.1103/PhysRevLett.58.1212.

[37] Yuxin Wang et al. “Thermoreflectance of metal transducers for time-domain thermoreflectance”. In: *Journal of Applied Physics* 108.043507 (2010). ISSN: 00218979. DOI: 10.1063/1.3457151.

[38] Roy M. Waxler and G.W. Cleek. “The effect of temperature and pressure on the refractive index of some oxide glasses”. In: *Journal of Research of the National Bureau*

of Standards Section A: Physics and Chemistry 77A.6 (2012), p. 755. ISSN: 0022-4332. DOI: 10.6028/jres.077a.046.

[39] A. J. Bosman and E. E. Havinga. "Temperature dependence of dielectric constants of cubic ionic compounds". In: *Physical Review* 129.4 (1963), pp. 1593–1600. ISSN: 0031899X. DOI: 10.1103/PhysRev.129.1593.

[40] J. Hohlfeld et al. "Electron and lattice dynamics following optical excitation of metals". In: *Chemical Physics* 251 (2000), pp. 237–258. ISSN: 03010104. DOI: 10.1016/S0301-0104(99)00330-4.